

Intramolecular π -stacking in cationic iridium(III) complexes with a triazole–pyridine type ancillary ligand: synthesis, photophysics, electrochemistry properties and piezochromic behavior†Guo-Gang Shan,^a Hai-Bin Li,^a Dong-Xia Zhu,^a Zhong-Min Su^{*a} and Yi Liao^{*b}

Received 25th January 2012, Accepted 8th April 2012

DOI: 10.1039/c2jm30480e

To make Ir(III)-based complexes potentially multifunctional materials, two new cationic Ir(III) complexes with a 2-(5-phenyl-2-phenyl-2H-1,2,4-triazol-3-yl)pyridine (**Phtz**) ancillary ligand were designed and synthesized. By introducing the pendant phenyl ring into the ancillary ligand, the two complexes possess desired intramolecular π - π stacking between the pendant phenyl ring of the **Phtz** ligand and one of the phenyl rings of the cyclometalated ligand, which renders the complexes more stable. Density functional theory calculation indicates that the intramolecular π - π interactions in both complexes can reduce the degradation reaction in metal-centered (³MC) states to some extent, which further implies their stability. With these results in combination with their reversible oxidation and reduction processes as well as excellent photophysical properties, the stable light-emitting cells (LECs) would be expected. Furthermore, the two synthesized complexes exhibit reversible piezochromism. Their emission color can be smartly switched by grinding and heating, which is visible to the naked eye. In light of our experimental results, the present piezochromic behavior is due to interconversion between crystalline and amorphous states.

Introduction

Phosphorescent transition-metal complexes (TMCs), particularly Ir(III) complexes, have attracted much attention due to their high emission efficiency, relatively long excited-state lifetime, photo- and thermal-stabilities, as well as easy tunability of the emission wavelength.¹ Therefore, Ir(III) complexes are promising for the various applications such as chemosensors,² biological probes,³ photocatalytic water reduction,⁴ organic light-emitting diodes (OLEDs)⁵ and light-emitting electrochemical cells (LECs).⁶ Ir(III)-based LECs, a new type of organic electroluminescent devices, possess several advantages over conventional OLEDs such as simple device architecture, low turn-on voltage, and independent of the work function of the electrode material, which are initial requirements for achieving the unencapsulated devices. Since Slinker reported the first LECs based on cationic Ir(III) complexes,⁷ Ir(III)-based LECs with green, yellow, orange and red emitting color have been achieved through careful

ligand-structure control.⁸ In addition, white LECs were realized *via* combination of blue-green and red emitting cationic Ir(III) complexes in a host–guest system.⁹ Nowadays, LECs are regarded as good candidates for potential flat-panel displays and low-cost solid-state lighting sources.

However, the water-assisted ligand-exchange reactions are believed to occur during the operations of LECs, resulting in luminescence quenching of emitting molecules, which remarkably decrease the efficiency and stability of the devices.¹⁰ Recent studies have demonstrated that the intramolecular π - π interactions between coordinated ligands within a single cationic Ir(III) complex significantly increase the stability of devices.¹¹ Although this approach has been presented, limited efforts have been devoted to designing and synthesizing the cationic Ir(III) complexes with intramolecular π -stacking up to now. To construct this kind of supramolecular interactions, the pendant phenyl ring was usually introduced into the appropriate position of the ancillary ligand. Recently, we reported two cationic Ir(III) complexes based on the 2-(5-methyl-2-phenyl-2H-1,2,4-triazol-3-yl)pyridine (**Mptz**) ancillary ligand.¹² By carefully analyzing the structure of the reported complex [Ir(dfppz)₂Mptz]PF₆ (dfppz: 1-(2,4-difluorophenyl)-1H-pyrazole), and replacing the methyl group of the ancillary ligand with a phenyl moiety, the intramolecular π -stacking conformation might be achieved in the designed complex. Furthermore, the complex **B1** also exhibited fascinating piezochromic property, which opens up the new opportunities for Ir(III) complexes in optical recording and

^aInstitute of Functional Material Chemistry, Faculty of chemistry, Northeast Normal University, Changchun, 130024 Jilin, People's Republic of China. E-mail: zmsu@nenu.edu.cn

^bDepartment of Chemistry, Capital Normal University, Beijing, People's Republic of China. E-mail: liaoy271@nenu.edu.cn

† Electronic supplementary information (ESI) available: ¹H NMR and MS spectra of complexes **1** and **2** and the calculational informations. CCDC 862865 (**1**) and 862866 (**2**). For ESI and crystallographic data in CIF or other electronic format see DOI: 10.1039/c2jm30480e

temperature- and pressure-sensing fields.¹³ Thereby, it is of great interest to design and synthesize an Ir(III) complex capable of possessing the intramolecular π -stacking structure and simultaneously exhibiting the reversible piezochromic property.

In this contribution, we designed and successfully synthesized two novel cationic Ir(III) complexes with the 2-(5-phenyl-2-phenyl-2*H*-1,2,4-triazol-3-yl)pyridine (**Phtz**) ancillary ligand, namely [Ir(dfppz)₂(Phtz)](PF₆) (**1**) and [Ir(ppy)₂(Phtz)](PF₆) (**2**) (Scheme 1) in which ppy was 2-phenylpyridine. Their X-ray crystal structures clearly demonstrated that they possessed the desired intramolecular π - π stacking between the pendant phenyl ring of the **Phtz** ligand and one of the phenyl rings of the cyclometalated ligand. The photophysical properties and their stability caused by these intramolecular π - π interactions were rationalized by theoretical calculations based on the density functional theory (DFT) approach. In particular, the complexes **1** and **2** also exhibited an interesting piezochromism, and the color changes in solid state emission could be repeated many times, indicative of an excellent reversibility in the switching processes.

Experimental section

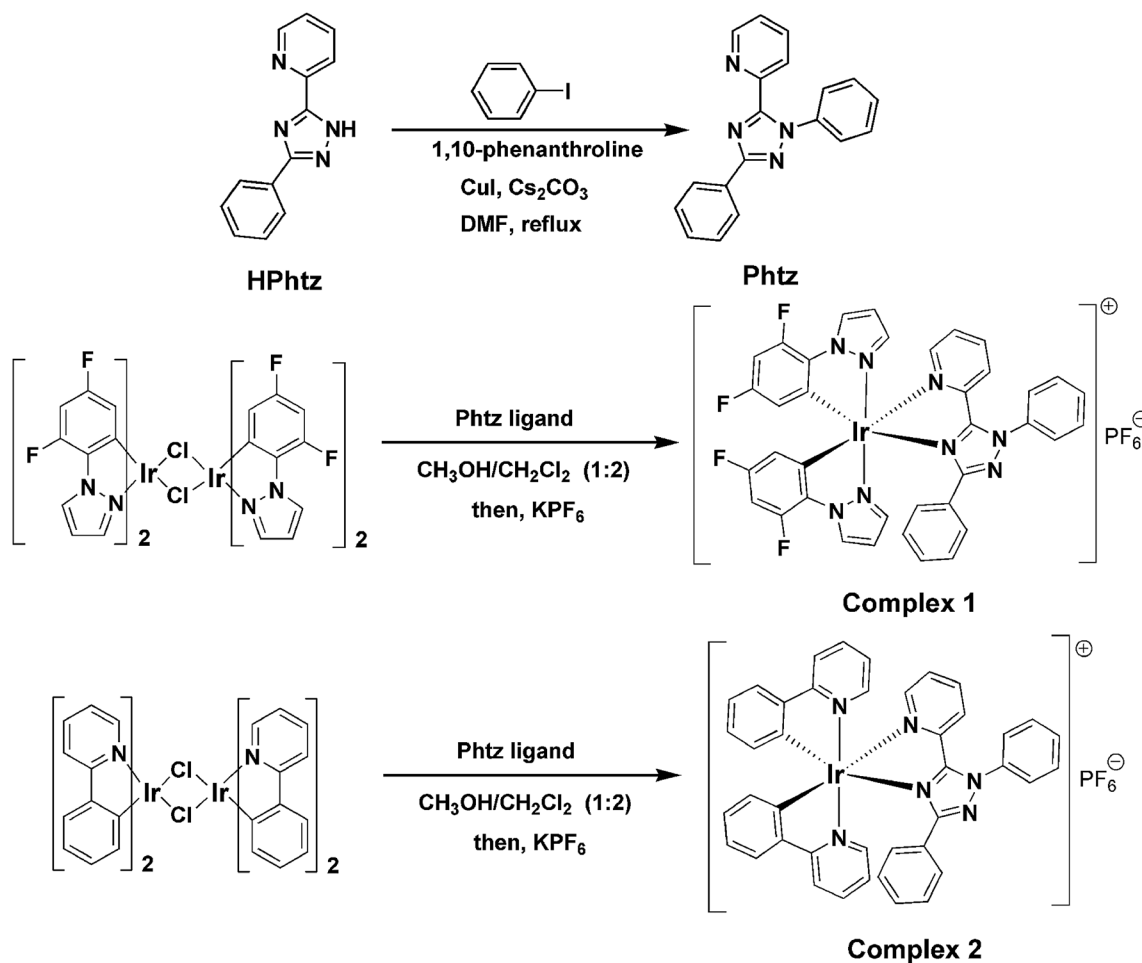
Materials and measurements

All reagents and solvents employed were commercially available and used as received without further purification. The solvents for

syntheses were freshly distilled over appropriate drying reagents. All experiments were performed under a nitrogen atmosphere by using standard Schlenk techniques. Elemental analyses (C, H, and N) were performed on a Perkin-Elmer 240C elemental analyzer. TG analyses were performed on a Perkin-Elmer TG-7 analyzer heated from 30 to 800 °C in a flow of nitrogen at the heating rate of 10 °C min⁻¹. Powder X-ray diffraction (XRD) patterns of the samples were collected on a Rigaku Dmax 2000. ¹H NMR spectra were measured on Bruker Avance 500 MHz with tetramethylsilane as the internal standard. The molecular weights of ligands and complexes were tested by using electrospray-ionization mass spectroscopy and matrix-assisted laser desorption-ionization time-of-flight (MALDI-TOF) mass spectrometry, respectively. UV-vis absorption spectra were recorded on a Hitachi U3030 spectrometer. The emission spectra were recorded using the F-7000 FL spectrophotometer. The excited-state lifetime was measured on a transient spectrofluorimeter (Edinburgh FLS920) with a time-correlated single-photo-counting technique. The photoluminescence quantum yields (PLQYs) of the neat film were measured in an integrating sphere.

Synthesis

The cyclometalated chloride-bridged dimers were synthesized according to a procedure described in the literature by refluxing



Scheme 1 Synthesis of the ancillary ligand (**Phtz**) and the cationic Ir(III) complexes **1** and **2**.

$\text{IrCl}_3 \cdot 3\text{H}_2\text{O}$ with the corresponding cyclometalated ligands in the mixture of 2-ethoxyethanol and water.¹⁴ The ancillary ligands **Phtz** were synthesized as depicted in Scheme 1. Complexes **1** and **2** could be readily achieved from the reaction of ancillary ligands with the organometallated dichloro-bridged dimer $[\text{Ir}(\text{dfppz})_2\text{Cl}]_2$ and $[\text{Ir}(\text{ppy})_2\text{Cl}]_2$, respectively, by a bridge-splitting reaction. The molecular structures of these complexes were characterized by ^1H NMR, mass spectrometry and elemental analysis (Fig. S1–S6, ESI†).

2-(5-Phenyl-2H-1,2,4-triazol-3-yl)pyridine (Phtz). The precursor 2-(5-phenyl-2H-1,2,4-triazol-3-yl)pyridine (HPhtz) (1.69 g, 7.6 mmol), iodobenzene (2.45 g, 12 mmol), 1,10-phenanthroline (0.96 g, 4.8 mmol), copper(I) iodide (0.48 g, 2.5 mmol), and caesium carbonate (3.72 g, 11 mmol) were dissolved in DMF (40 mL). The mixture was stirred vigorously for 10 min at room temperature (RT) and subsequently refluxed under an argon atmosphere for another 24 h. After cooling to RT, the solvent was removed under vacuum, then the residue was extracted with CH_2Cl_2 (200 mL). The product was then obtained by column chromatography on silica gel with petroleum ether (b.p. 60–90 °C)–ethyl acetate (2 : 1) as the eluent to yield a white solid (75%). ^1H NMR (500 MHz, CDCl_3 , ppm): δ 8.52–8.53 (m, 1H), 8.25–8.27 (m, 1H), 7.93–7.94 (m, 1H), 7.77–7.81 (m, 1H), 7.42–7.50 (m, 8H), 7.30–7.33 (m, 1H). Anal. calcd for $\text{C}_{19}\text{H}_{14}\text{N}_4$: C, 76.49; H, 4.73; N, 18.78. Found: C, 76.52; H, 4.81, N, 18.83%. ESI-MS (m/z): 299.1307 $[\text{M} + \text{H}]^+$.

$[\text{Ir}(\text{dfppz})_2(\text{Phtz})](\text{PF}_6)$ (1**).** A solution of ligand **Phtz** (0.63 g, 2.1 mmol) and the dichloro-bridged diiridium complex $[\text{Ir}(\text{dfppz})\text{Cl}]_2$ (1.2 g, 1.0 mmol) in dichloromethane (30 mL) and methanol (15 mL) was refluxed for 24 h in the dark. After cooling to room temperature, the mixture was filtrated, and then an excess of solid KPF_6 was added and stirred for another 0.5 h at room temperature. The solvent was removed under reduced pressure and the residue was purified by silica gel column chromatography using ethyl acetate to yield **1**. (72%). ^1H NMR (500 MHz, d_6 -DMSO, ppm): δ 8.66 (d, $J = 2.5$ Hz, 1H), 8.55 (d, $J = 2.5$ Hz, 1H), 8.15 (t, $J = 8$ Hz, 1H), 8.05 (d, $J = 2.5$ Hz, 1H), 8.01 (d, $J = 5.5$ Hz, 1H), 7.92 (d, $J = 6.5$ Hz, 2H), 7.79–7.83 (m, 3H), 7.69 (t, $J = 6$ Hz, 1H), 7.57 (d, $J = 2.5$ Hz, 1H), 7.35 (d, $J = 8$ Hz, 1H), 7.27–7.30 (m, 1H), 7.08–7.15 (m, 5H), 6.90 (t, $J = 3$ Hz, 1H), 6.86 (t, $J = 3$ Hz, 1H), 6.68–6.73 (m, 1H), 5.55–5.57 (m, 1H), 5.12–5.14 (m, 1H). Anal. calcd for $\text{IrC}_{37}\text{H}_{24}\text{N}_8\text{F}_{10}\text{P}$: C, 44.72; H, 2.43; N, 11.28. Found: C, 44.76; H, 2.51, N, 11.39%. MS (MALDI-TOF): m/z 849.2 (M – PF_6).

$[\text{Ir}(\text{ppy})_2(\text{Phtz})](\text{PF}_6)$ (2**).** The synthesis of complex **2** was similar to that of complex **1** except that the organometallated dimer 1-(2,4-difluorophenyl)-1H-pyrazole (dfppz) was replaced with 2-phenylpyridine (ppy). The crude product was also purified by silica gel column chromatography using ethyl acetate as eluent. ^1H NMR (500 MHz, d_6 -DMSO, ppm): δ 8.54 (d, $J = 5$ Hz, 1H), 8.31 (d, $J = 8$ Hz, 1H), 7.98–8.09 (m, 3H), 7.77–7.95 (m, 9H), 7.63–7.66 (m, 1H), 7.46 (d, $J = 6.5$ Hz, 1H), 7.31–7.34 (m, 2H), 7.16–7.25 (m, 4H), 6.98–7.01 (m, 1H), 6.93 (t, $J = 8$ Hz, 1H), 6.83–6.86 (m, 1H), 6.63–6.71 (m, 2H), 6.07 (d, $J = 7.5$ Hz, 1H), 5.95 (d, $J = 7.5$ Hz, 1H). Anal. calcd for $\text{IrC}_{41}\text{H}_{30}\text{N}_6\text{F}_6\text{P}$: C,

52.17; H, 3.20; N, 8.90. Found: C, 52.20; H, 3.25, N, 8.92%. MS (MALDI-TOF): m/z 799.2 (M – PF_6).

X-ray crystallography study

Data collection of complexes **1** and **2** was performed on a Bruker Smart Apex II CCD diffractometer with graphite-monochromated Mo K_α radiation ($\lambda = 0.71069$ Å) at 293 K. Absorption corrections were performed by using the multi-scan technique. The crystal structure was solved by Direct Methods of SHELXTL-97 (ref. 16) and refined by full-matrix least-squares techniques using SHELXTL-97 within WINGX.¹⁷ The hydrogen atoms of aromatic rings were included in the structure factor calculation at idealized positions by using a riding model. Anisotropic thermal parameters were used to refine all non-hydrogen atoms except for some of the nitrogen and carbon atoms. The detailed crystallographic data and structure refinement parameters are summarized in Table S1 (ESI†).

Electrochemical measurements

Cyclic voltammetry was performed on a BAS 100 W instrument with a scan rate of 100 mV s^{-1} in CH_3CN (10^{-3} M) with the three-electrode configuration: a glassy-carbon electrode as the working electrode, an aqueous saturated calomel electrode as the pseudo-reference electrode, and a platinum wire as the counter-electrode. A 0.1 M solution of tetrabutylammonium perchlorate (TBAP) in CH_3CN was used as the supporting electrolyte and ferrocene was selected as the internal standard.

Theoretical calculations

The ground and excited electronic states of complexes were investigated by performing DFT and TD-DFT calculations at the B3LYP level.¹⁸ The 6-31G* basis sets were employed for optimizing the C, H, N atoms and the LANL2DZ basis sets for the Ir atom. An effective core potential (ECP) replaces the inner core electrons of iridium leaving the outer core $(5s)^2(5p)^6$ electrons and the $(5d)^6$ valence electrons of Ir(III). The geometry of the metal-centered triplet (^3MC) was fully optimized and was calculated at the spin-unrestricted UB3LYP level with a spin multiplicity of 3. All calculations reported here were carried out with the Gaussian 09 software package.¹⁹

Results and discussion

X-ray structure characterization

Crystal structures of **1** and **2** were obtained by the slow evaporation of diethyl ether into the CH_2Cl_2 solution. As depicted in Fig. 1, both complexes reveal the distorted octahedral geometry around the Ir atom with two cyclometalated ligands and one ancillary ligand. Both the cyclometalated ligands adopt a mutually eclipsed configuration with two nitrogen atoms residing at *trans* locations. The overall structural arrangement is similar to several previously reported ones.^{8b,9b,11a,20} Moreover, the bond length $\text{Ir}-\text{N}_{\text{ancillary ligand}}$ is significantly longer than that of $\text{Ir}-\text{N}_{\text{cyclometalated ligand}}$, which might be attributed to the strong *trans* influence of the carbon donors.²¹ For example, in the case of complex **1**, the Ir–N bond lengths in the ancillary ligand Ir1–N5

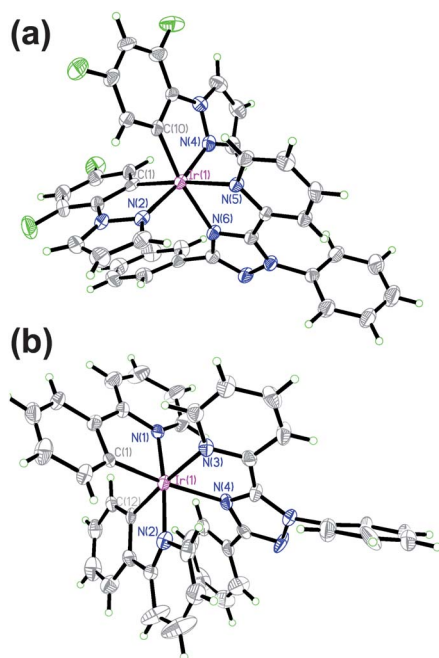


Fig. 1 Crystal structure of complexes **1** (a) and **2** (b). Thermal ellipsoids are drawn at 30% probability. The PF₆ counter-anion is omitted for clarity.

and Ir1–N6 are 2.161(3) Å and 2.145(4) Å, respectively, which are longer than those in the cyclometalated ligand Ir1–N2 (2.028(4) Å) and Ir1–N4 (2.018(4) Å) (see Table S2, ESI†). In addition, the bite angles of the **Phtz** ligands (75.98(14)° for **1** and 76.00(3) and 75.50(3)° for **2**) are smaller than those of the cyclometalated ligands (80.02(19) and 80.26(19)° for **1** and 80.30(3), 79.60(3), 81.40(4) and 79.30(4)° for **2**). These observations have also been made in related cationic Ir(III) complexes.²² As expected, the robust π – π stacking between the phenyl ring of the **Phtz** ligand and phenyl ring of one of the cyclometalated ligands is observed in complex **1**, with a centroid–centroid distance of *ca.* 3.6 Å (Fig. 2a). Although there are two isolated complexes **2** in the crystal structures, the intramolecular π – π interactions are also constructed (see Fig. 2b and S7, ESI†). This observation confirms our hypothesis that with replacement of the methyl group of complex [Ir(dfppz)₂Mptz]PF₆ with a phenyl substituent, the supramolecular cage configuration is formed. The inherent intramolecular π – π interactions in both complexes should reduce the possibility for nucleophilic attack, and thus stable LECs could be obtained *via* such complexes.¹¹

Photophysical properties

The absorption and emission spectra recorded for **1** and **2** in degassed CH₃CN at room temperature are shown in Fig. 3. The detailed photophysical characteristics are summarized in Table 1. As shown in Fig. 3, both complexes exhibit two major absorption bands in their absorption spectra. The dominant absorption band in the range of 200–350 nm is assigned to spin-allowed π – π^* transitions from the ligands. The low-energy absorption from 350 nm extending to the visible region is ascribed to both spin-allowed, spin-forbidden metal-to-ligand charge transfer (³MLCT) and ligand-to-ligand charge transfer (¹LLCT)

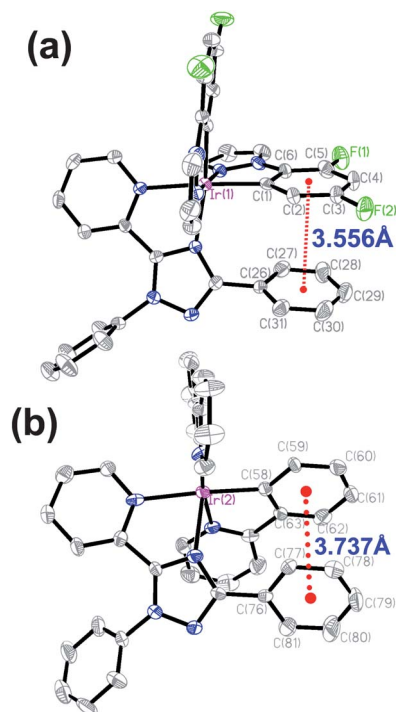


Fig. 2 The intramolecular π – π interactions are shown in **1** (a) and **2** (b), respectively.

character with reference to that reported for other Ir(III) complexes.^{6,8,23} Generally, for cationic Ir(III) complexes, three excited states contribute to the observation of light emission, namely, LC ³ π – π^* , ³MLCT and ³LLCT. The emission spectra from the ³MLCT state are usually broad and featureless, while the obvious structured emission bands are always attributed to the LC ³ π – π^* state.²⁴ At room temperature, both complexes display almost featureless emission spectra in solutions and neat film, indicating that their emissive excited states take on much more ³MLCT or ³LLCT characters than LC ³ π – π^* characters (Fig. 3, S8 and S9, ESI†). In the neat film, emission peaks of **1** and **2** occurred at 499 and 564 nm, respectively, with a quantum efficiency of 0.18 for **1** ($\tau = 0.57$ μ s) and 0.25 for **2** ($\tau = 0.20$ μ s).

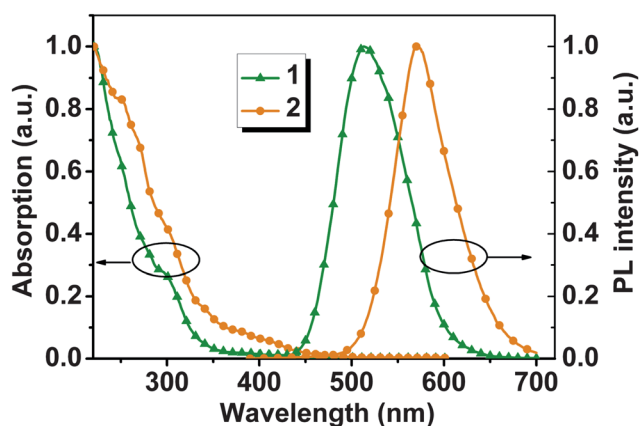


Fig. 3 Normalized absorption and emission spectra of complexes **1** and **2** in the CH₃CN solvent at room temperature.

Table 1 Photophysical and electrochemical characteristics of complexes **1** and **2**

Emission at room temperature			Emission at 77 K	Electrochemical data ^c	
Solution λ [nm]	Neat film λ [nm]	Φ_{em}^a (τ [μ s])	λ^b [nm]	$E_{ox}^{1/2}$ (V)	$E_{red}^{1/2}$ (V)
1 513 (CH ₃ CN) 504 (CH ₂ Cl ₂)	499	0.18 (0.57)	479	1.27	-1.41
2 570 (CH ₃ CN) 568 (CH ₂ Cl ₂)	564	0.25 (0.20)	511	0.89	-1.42

^a Measured in the neat film. ^b In CH₃CN glass. ^c The data were *versus* Fc^{+/}Fc (Fc is ferrocene).

The relatively high PLQY in neat film is beneficial for the application in optical devices. Upon cooling the CH₃CN solutions to 77 K, their emission spectra undergo rigidochromic blue shifts, but still are broad and featureless (Fig. S8, ESI†). These emission properties at 77 K further suggest that their emissions mainly originate from ³MLCT mixed with ³LLCT states.²⁵ It is noticeable that after replacing the cyclometalated ligand 1-(2,4-difluorophenyl)-1*H*-pyrazole (dfppz) with the 2-phenylpyridine (ppy) ligand, the emission of **2** is red-shifted compared to the green emission of the complex **1**, which can be attributed to the decreased HOMO levels. This viewpoint is firmly supported by their electrochemical behaviors.

Electrochemical properties

The electrochemical behaviors of complexes **1** and **2** were investigated by cyclic voltammetry in CH₃CN solution, and the redox potentials are listed in Table 1. Both complexes exhibit reversible oxidation and reduction processes in CH₃CN solution. The redox reversibility indicates that both the holes (upon oxidation) and electrons (upon reduction) can be easily transported and is beneficial for the application of the complexes in LECs.²⁶ Because the reduction of the cationic Ir(III) complexes usually occurs on the ancillary ligands, the reduction potential of complex **1** (-1.41) is almost identical to that of **2** (-1.42). As the π - π^* energy gap of the cyclometalated ligand decreases from complex **1** to complex **2**, the oxidation potentials are shifted anodically (Table 1), indicating that the HOMO energy level of **1** was stabilized with respect to that of complex **2**. Thus, the energy gap of **1** should be larger than that of **2**, which is in agreement with our photophysical data (*vide supra*).

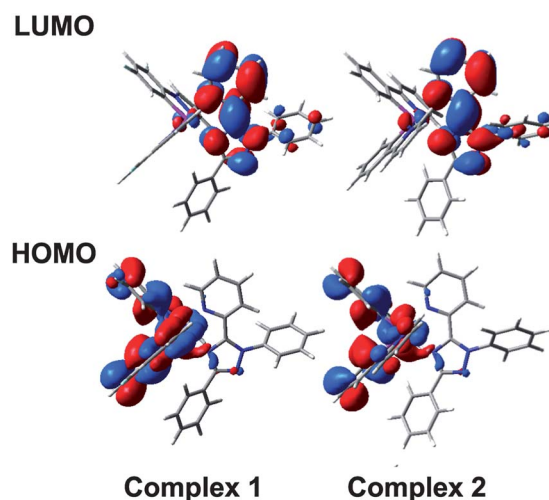
Quantum chemical calculations

To gain insight into the nature of the emissive excited state involved in the emission process of complexes **1** and **2**, the quantum chemical calculations were performed (see Experimental section). The low-lying triplet states of both complexes are calculated based on their optimized ground geometry through a time-dependent density functional theory approach (TD-DFT). The excitation energies and molecular orbitals involved in the excitations are summarized in Fig. 4 and Table S3 (ESI†).

According to our quantum chemical calculation results, the LUMOs of **1** and **2** are almost identical which reside on the

pyridine and 1,2,4-triazol groups of ancillary ligand. Two phenyl rings in ancillary ligand have not contributed to the LUMO orbitals. Their HOMOs mainly localize on the cyclometalated ligands and d orbital of iridium atom. On the basis of the TD-DFT calculation and orbital diagrams, the T₁ states of the two complexes originate from the excitation of HOMO \rightarrow LUMO (91% and 95% for complexes **1** and **2**, respectively), with character of mixed ³MLCT (Ir atom \rightarrow pyridine and 1,2,4-triazol groups of ancillary ligands) and ³LLCT (cyclometalated ligands \rightarrow pyridine and 1,2,4-triazol groups of ancillary ligands). According to the photophysical results, it is believed that the observed emission bands of both complexes should mainly originate from the ³MLCT (Ir \rightarrow ancillary ligands) and ³LLCT (cyclometalated ligands \rightarrow ancillary ligands) states. The quantum chemical calculations therefore indicate that the nature of the emissive excited state of complexes **1** and **2** could be attributed to the mixed ³MLCT and ³LLCT characters with different contributions.

In addition, the metal-centered states (³MC) result from the excitation of an electron from the occupied t_{2g}(d π) HOMO to the unoccupied e_g(d σ^*), which is assigned to be the origin of the degradation process for the Ru(II)- and Ir(III)-based LECs.^{10b,11b,27} In light of the experimental and theoretical results, Bolink *et al.* have demonstrated that the metal–ligand bond length in the ³MC state played a key role for the stability of the Ir(III)-based LECs.^{11c} The rupture of metal–ligand bonds can open the structure of the complexes and enhance the reactivity of complexes in the ³MC state, facilitating the degradation process and resulting in unstable LECs. However, the cage effect caused by the intramolecular π - π interaction effectively restricts the opening of the structure of complexes in the ³MC state, leading to the virtual decoordination of only one of the N_{cyclometalated ligand} atoms. This supramolecular cage effect makes the cationic Ir(III) complexes more robust, reducing the possibility of the ligand-exchange degradation reaction. To determine whether the intramolecular π - π interactions in complexes **1** and **2** can reduce the opening of structures in the ³MC state or not, the geometry optimization of their ³MC states has been performed following the methodology illustrated in the reported works.^{10b,28} The metal-centered

**Fig. 4** Calculated HOMO and LUMO orbitals for complexes **1** and **2**.

characters of the triplet state for both complexes **1** and **2** were confirmed by the spin densities calculated for the optimized ^3MC states geometries (see Fig. S10, ESI†). The spin densities are mainly concentrated on the iridium atom, and hold 1.50 and 1.50 unpaired electrons for complexes **1** and **2** in ^3MC states, respectively. As shown in Fig. 5, the Ir–N bond (R1) of the cyclometalated ligands in complexes **1** (**2**) involved in the π – π interaction only lengthens from 2.08 Å (2.08 Å) in ground states (S_0) to 2.17 Å (2.23 Å) in the ^3MC state. In contrast, electron promotion results in the elongation of another two Ir–N_{cyclometalated ligand} lengths (R2), from 2.05 Å in S_0 state to 2.50 Å in ^3MC state for **1**, and from 2.08 Å in S_0 state to 2.52 Å in ^3MC state for **2**, respectively. Consequently, the π – π interactions in both complexes (**1** and **2**) would be in favor for reducing the degradation reaction in ^3MC to some extent and precluding the attack by the nucleophiles, which is very beneficial for LECs.

Piezochromic behavior

Interestingly, the solid state powders of complexes **1** and **2** obtained through column chromatography exhibit unusual piezochromic behaviors. For clarity, the as-synthesized samples, ground and heated ground samples, were hereafter abbreviated as the letters “A”, “G” and “H”, respectively (e.g., the sample **1A** is the as-synthesized complex **1** through column chromatography; **1G** is the ground sample of **1A**). Upon grinding, the emission color changes of samples **1A** and **2A** are depicted in Fig. 6, showing a significant emission red-shift from sky-blue to blue-green for **1A** and from yellow to orange for **2A**, respectively. In addition, the experimental results show that the solid-state absorption spectra are different between the as-synthesized samples and ground samples. As shown in Fig. S11†, the absorption spectra of the ground samples **1G** and **2G** were obviously red-shifted and broadened compared with those of the as-synthesized samples **1A** and **2A**, respectively, indicating that the changes in the emission color may be caused by changing the mode of the molecular packing. Here, we take complex **1** as an example. When the sky-blue emitting ($\lambda_{\text{max}} = 471 \text{ nm}$, $0.94 \mu\text{s}$) solid state powder **1A** was ground, the obtained sample **1G** emitted blue-green luminescence at 499 nm with the lifetime being $1.0 \mu\text{s}$ (Fig. 7a). Similar to **1A**, the samples **2A** also exhibit a pressure-induced luminescence change feature, with the emission wavelength changing from 542 nm ($0.70 \mu\text{s}$) to 563 nm ($0.50 \mu\text{s}$) upon grinding treatment. The change in emission maximum of **1A** and **2A** before and after grinding are 28 and 21 nm,

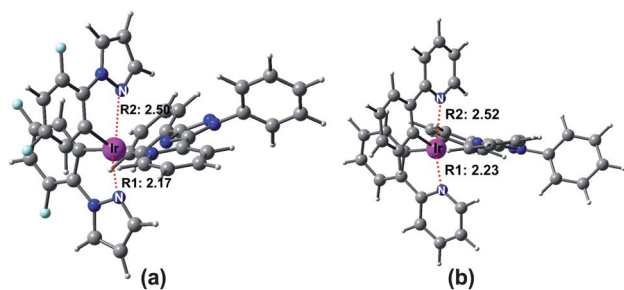


Fig. 5 The minimum-energy structure calculated for the ^3MC state of complexes **1** (a) and **2** (b), respectively. Ir–N_{cyclometalated ligand} bond lengths are give in Å.

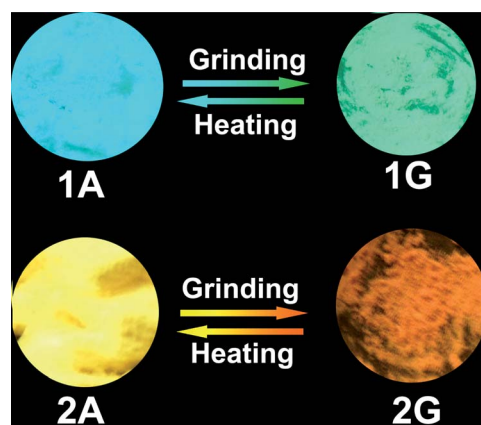


Fig. 6 Stimuli-responsive behaviors of as-synthesized complexes **1A** and **2A** upon grinding and heating treatments (under UV lamp, $\lambda_{\text{ex}} = 365 \text{ nm}$).

respectively. Evidently, the complexes **1** and **2** are piezochromic materials. Interestingly, the emission color of the ground samples **1G** and **2G** can easily be reverted to the original unground state (**1A** and **2A**) upon heating at $230 \text{ }^\circ\text{C}$ for 5 min (Fig. S12, ESI†). When the heated samples **1H** and **2H** were further ground, the blue-green and orange-emitting powders were obtained again. These color changes in solid state emission of **1A** and **2A** are thus repeated many times, indicative of an excellent reversibility in the switching processes (Fig. 8). To verify the change in the chemical structure of samples **1A** and **2A** in different states, their ^1H NMR and MALDI-TOF spectra have been determined. The spectra in different states are almost identical (Fig. S13 and S14, ESI†), indicating that their different emission properties might be caused by physical processes, such as changing the

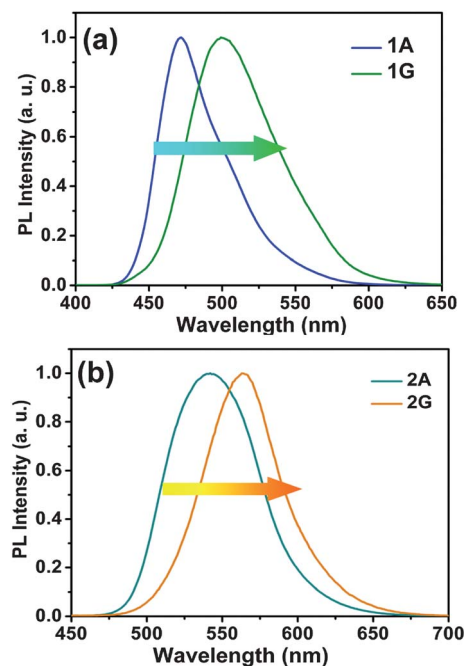


Fig. 7 The emission spectra of unground and ground samples **1A** (a) and **2A** (b).

intermolecular interactions and/or the mode of the molecular packing during the grinding and heating processes. It is important to point out that a strong shift in emission color was also observed by Bolink *et al.*²⁹ for a cationic Ir(III) complex in thin films with different concentrations and the associated LECs, which is detrimental for cationic Ir(III) complexes as blue-emitting LECs. It is believed that the reported reversible piezochromic effect will be helpful for preparing rare blue-emitting Ir(III)-based LECs through appropriate treatments and further developing white-light emitting applications. In addition, when the powders **1A** and **2A** were spread on the filter paper, the letters "IFMC" were written on them with a spatula, respectively. Under the UV lamp, the marked "IFMC" can be observed clearly on the sky-blue and yellow "paper" with the naked eye (Fig. S15, ESI†), implying that both **1A** and **2A** have potential application in the fields of optical recording and pressure-sensing.

The mechanism for the present piezochromic behavior

To determine the possible mechanism of the present piezochromic behavior, the powder X-ray diffraction (PXRD) measurements were performed on each sample (Fig. 9a and b). PXRD patterns measured for **1A** and **2A** are in agreement with the simulated results from the respective single crystal XRD data. These intensive and sharp reflection peaks were observed in the samples **1A** and **2A**, indicating that **1A** and **2A** should be the well-ordered aggregates.³⁰ In contrast, the obtained ground samples **1G** and **2G** show very weak and broad diffraction signal intensities, indicating that the amorphous states formed instead of the original ordered structures. The small peaks in the XRD patterns of **1G** and **2G** with the 2θ values consistent with those of the peaks for **1A** and **2A** implied that a part of unground samples **1A** and **2A** remained after grinding. This result suggests that their piezochromic behavior is generated *via* changing the model of molecular packing upon grinding, such as from crystalline state to amorphous state. Generally, the amorphous solid will become less viscous and the molecules may obtain enough freedom of motion to spontaneously arrange themselves into a crystalline form upon heating. Herein, the ground samples were heated at 230 °C for 5 min, some sharp diffraction peaks appeared and these peaks coincided with those of corresponding unground crystals (Fig. 9a and b). It suggests that the difference in XRD patterns from samples **1G** and **2G** to samples **1H** and **2H** is ascribed to the transition from amorphous ground samples to the crystalline states after heat treatment. Except heating treatment, recrystallization is another feasible approach to make the

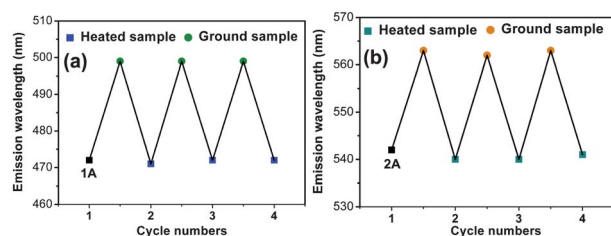


Fig. 8 Emission wavelengths of the repeated piezochromic behaviors of **1A** (a) and **2A** (b).

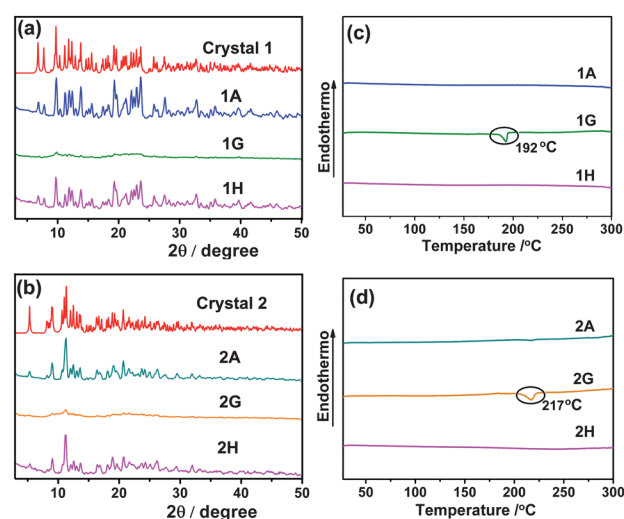


Fig. 9 Power X-ray diffraction patterns of **1A** (a) and **2A** (b) in different state, and the DSC curves of the corresponding samples of **1A** (c) and **2A** (d) in different state.

amorphous phase samples (**1G** and **2G**) revert to the crystalline state samples. Similar results were also observed for other reported piezochromic material.³¹ As shown in Fig. S16 and S17 (ESI†), the XRD patterns and emission spectra of recrystallized samples perfectly reverted to the original crystalline states.

In addition, the thermal properties of all samples obtained from different treatments are carefully analyzed by differential scanning calorimetry (DSC). In the DSC curves of the heating of unground (**1A** and **2A**) and heated samples (**1G** and **2G**), there are no endo- and/or exo-thermic peaks prior to 300 °C (see Fig. 9c and d). In contrast, upon heating amorphous states **1G** and **2G**, their DSC curves exhibit an exothermic recrystallization peak at temperatures about 192 °C and 217 °C for **1G** and **2G**, respectively. The observed recrystallization peaks of ground samples and the transition enthalpy (see Table S4†) suggest that the ground samples are a metastable state which can be restored to thermodynamically stable crystals (**1A** and **2A**) from the powders (**1G** and **2G**) through an exothermic recrystallization process.

Conclusion

In summary, two cationic complexes possessing the intramolecular π - π stacking between **Phtz** ancillary ligands and one of the cyclometalated ligands and exhibiting interesting piezochromic property were designed and successfully prepared. Studies on their photophysical properties in solution and films have been carried out. Both complexes showed intense emission in both solution and neat film, and their emission mechanism has been supported by the quantum chemical calculations. Our theoretical results also indicated that this supramolecular cage effect made both complexes more robust, which reduced the possibility of the ligand-exchange degradation reaction and resulted in stable complexes even in ³MC states. Furthermore, both complexes exhibited the fascinating piezochromic phosphorescence properties in solid state with an obvious change in emission color which was visible to the naked eye. The reversible

piezochromic phosphorescence nature is attributed to a crystal-line-amorphous phase transformation by carefully analyzing their PXRD, DSC and ^1H NMR data in different states. We believe that this reversible color change feature and robust π - π intramolecular interactions can make them useful in fabricating stable LECs and optical recording applications in future.

Acknowledgements

The authors gratefully acknowledge financial support from NSFC (20971020, 20903020 and 21131001), 973 Program (2009CB623605), and the Science and Technology Development Planning of Jilin Province (20100540 and 201101008).

Notes and references

- (a) C. Ulbricht, B. Beyer, C. Friebe, A. Winter and U. S. Schubert, *Adv. Mater.*, 2009, **21**, 4418; (b) Y. M. You and S. Y. Park, *Dalton Trans.*, 2009, 1267.
- (a) Q. Zhao, F. Y. Li and C. H. Huang, *Chem. Soc. Rev.*, 2010, **39**, 3007; (b) H. Y. Shiu, M. K. Wong and C. M. Che, *Chem. Commun.*, 2011, **47**, 4367; (c) G. G. Shan, D. X. Zhu, H. B. Li, P. Li, Z. M. Su and Y. Liao, *Dalton Trans.*, 2011, **40**, 2947; (d) Y. M. You and S. Y. Park, *Adv. Mater.*, 2008, **20**, 3820.
- (a) D. L. Ma, W. L. Wong, W. H. Chung, F. Y. Chan, P. K. So, T. S. Lai, Z. Y. Zhou, Y. C. Leung and K. Y. Wong, *Angew. Chem., Int. Ed.*, 2008, **47**, 3735; (b) K. K. W. Lo, K. Y. Zhang, S. K. Leung and M. C. Tang, *Angew. Chem., Int. Ed.*, 2008, **47**, 2213; (c) K. Y. Zhang, S. P. Y. Li, N. Y. Zhu, I. W. S. Or, M. S. H. Cheung, Y. W. Lam and K. K. W. Lo, *Inorg. Chem.*, 2010, **49**, 2530.
- (a) M. S. Lowry and S. Bernhard, *Chem.–Eur. J.*, 2006, **12**, 7970; (b) E. D. Cline, S. E. Adamson and S. Bernhard, *Inorg. Chem.*, 2008, **47**, 10378.
- (a) J. Q. Ding, B. Wang, Z. Y. Yue, B. Yao, Z. Y. Xie, Y. X. Cheng, L. X. Wang, X. B. Jing and F. S. Wang, *Angew. Chem., Int. Ed.*, 2009, **48**, 6664; (b) Y. C. Chiu, J. Y. Hung, Y. Chi, C. C. Chen, C. H. Chang, C. C. Wu, Y. M. Cheng, Y. C. Yu, G. H. Lee and P. T. Chou, *Adv. Mater.*, 2009, **21**, 2221; (c) B. Ma, B. J. Kim, D. A. Poulsen, S. J. Pastine and J. M. J. Fréchet, *Adv. Funct. Mater.*, 2009, **19**, 1024; (d) J. J. Kim, Y. You, Y. S. Park, J. J. Kim and S. Y. Park, *J. Mater. Chem.*, 2009, **19**, 8347; (e) Y. T. Tao, Q. Wang, C. L. Yang, K. Zhang, Q. Wang, T. T. Zou, J. G. Qin and D. G. Ma, *J. Mater. Chem.*, 2008, **18**, 4091; (f) S. Bettington, M. Tavasli, M. R. Bryce, A. S. Batsanov, A. L. Thompson, H. A. Al Attar, F. B. Dias and A. P. Monkman, *J. Mater. Chem.*, 2006, **16**, 1046; (g) S. C. Lo, R. E. Harding, C. P. Shipley, S. G. Stevenson, P. L. Burn and I. D. W. Samuel, *J. Am. Chem. Soc.*, 2009, **131**, 16681.
- (a) M. Mydlak, C. Bizzarri, D. Hartmann, W. Sarfert, G. Schmid and L. De Cola, *Adv. Funct. Mater.*, 2010, **20**, 1812; (b) M. K. Nazeeruddin, R. T. Wegh, Z. Zhou, C. Klein, Q. Wang, F. D. Angelis, S. Fantacci and M. Grätzel, *Inorg. Chem.*, 2006, **45**, 9245; (c) W. Y. Wong, G. J. Zhou, X. M. Yu, H. S. Kwok and Z. Y. Lin, *Adv. Funct. Mater.*, 2007, **17**, 315; (d) R. D. Costa, E. Ortí, H. J. Bolink, S. Graber, S. Schaffner, M. Neuburger, C. E. Housecroft and E. C. Constable, *Adv. Funct. Mater.*, 2009, **19**, 3456; (e) T. H. Kwon, Y. H. Oh, I. S. Shin and J. I. Hong, *Adv. Funct. Mater.*, 2009, **19**, 711.
- J. D. Slinker, A. A. Gorodetsky, M. S. Lowry, J. J. Wang, S. Parker, R. Rohl, S. Bernhard and G. G. Malliaras, *J. Am. Chem. Soc.*, 2004, **126**, 2763.
- (a) C. Rothe, C. J. Chiang, V. Jankov, K. Abdullah, X. S. Zeng, R. Jitchati, A. S. Batsanov, M. R. Bryce and A. P. Monkman, *Adv. Funct. Mater.*, 2009, **19**, 2038; (b) J. M. Fernández-Hernández, C. H. Yang, J. I. Beltrán, V. Lemaire, F. Polo, R. Fröhlich, J. Cornil and L. De Cola, *J. Am. Chem. Soc.*, 2011, **133**, 10543; (c) R. D. Costa, F. J. Céspedes-Guirao, E. Ortí, H. J. Bolink, J. Gierschner, F. Fernández-Lázaro and A. Sastre-Santos, *Chem. Commun.*, 2009, 3386; (d) A. B. Tamayo, S. Garon, T. Sajoto, P. I. Djurovich, I. M. Tsyba, R. Bau and M. E. Thompson, *Inorg. Chem.*, 2005, **44**, 8723; (e) H. Su, C. Wu, F. Fang and K. Wong, *Appl. Phys. Lett.*, 2006, **89**, 261118.
- (a) L. He, L. Duan, J. Qiao, G. F. Dong, D. Q. Zhang, L. D. Wang and Y. Qiu, *Adv. Funct. Mater.*, 2009, **19**, 2950; (b) H. C. Su, H. F. Chen, F. C. Fang, C. C. Liu, C. C. Wu, K. T. Wong, Y. H. Liu and S. M. Peng, *J. Am. Chem. Soc.*, 2008, **130**, 3413; (c) L. He, L. Duan, J. Qiao, G. F. Dong, L. D. Wang and Y. Qiu, *Chem. Mater.*, 2010, **22**, 3535.
- (a) H. J. Bolink, L. Cappelli, E. Coronado, M. Grätzel, E. Ortí, R. D. Costa, P. M. Viruela and M. K. Nazeeruddin, *J. Am. Chem. Soc.*, 2006, **128**, 14786; (b) R. D. Costa, E. Ortí, H. J. Bolink, S. Graber, C. E. Housecroft and E. C. Constable, *Adv. Funct. Mater.*, 2010, **20**, 1511.
- (a) L. He, L. Duan, J. Qiao, D. Q. Zhang, L. D. Wang and Y. Qiu, *Chem. Commun.*, 2011, **47**, 6467; (b) H. J. Bolink, E. Coronado, R. D. Costa, E. Ortí, M. Sessolo, S. Graber, K. Doyle, M. Neuburger, C. E. Housecroft and E. C. Constable, *Adv. Mater.*, 2008, **20**, 3910; (c) R. D. Costa, E. Ortí, H. J. Bolink, S. Graber, C. E. Housecroft and E. C. Constable, *Chem. Commun.*, 2011, **47**, 3207.
- G. G. Shan, H. B. Li, H. T. Cao, D. X. Zhu, P. Li, Z. M. Su and Y. Liao, *Chem. Commun.*, 2012, **48**, 2000.
- (a) Y. Sagara and T. Kato, *Nat. Chem.*, 2009, **1**, 605; (b) J. Luo, L. Y. Li, Y. L. Song and J. Pei, *Chem.–Eur. J.*, 2011, **17**, 10515; (c) J. Kunzleman, M. Kinami, B. R. Crenshaw, J. D. Protasiewicz and C. Weder, *Adv. Mater.*, 2008, **20**, 119; (d) A. L. Balch, *Angew. Chem., Int. Ed.*, 2009, **48**, 2641; (e) G. Q. Zhang, J. W. Lu, M. Sabat and C. L. Fraser, *J. Am. Chem. Soc.*, 2010, **132**, 2160; (f) D. P. Yan, J. Lu, J. Ma, S. H. Qin, M. Wei, D. G. Evans and X. Duan, *Angew. Chem., Int. Ed.*, 2011, **50**, 7037; (g) S. J. Yoon, J. W. Chung, J. Gierschner, K. S. Kim, M. G. Choi, D. Kim and S. Y. Park, *J. Am. Chem. Soc.*, 2010, **132**, 13675; (h) H. Y. Li, Z. G. Chi, B. J. Xu, X. Q. Zhang, X. F. Li, S. W. Liu, Y. Zhang and J. R. Xu, *J. Mater. Chem.*, 2011, **21**, 3760.
- (a) E. Baranoff, S. Fantacci, F. D. Angelis, X. X. Zhang, R. Scopelliti, M. Grätzel and M. K. Nazeeruddin, *Inorg. Chem.*, 2011, **50**, 451; (b) G. G. Shan, L. Y. Zhang, H. B. Li, S. Wang, D. X. Zhu, P. Li, C. G. Wang, Z. M. Su and Y. Liao, *Dalton Trans.*, 2012, **41**, 523.
- E. Orselli, G. S. Kottas, A. E. Konradsson, P. Coppo, R. Fröhlich, L. De Cola, A. van Dijken, M. Büchel and H. Börner, *Inorg. Chem.*, 2007, **46**, 11082.
- G. M. Sheldrick, *SHELXL-97, Program for Crystal Structure Refinement*, University of Göttingen, 1997.
- L. J. Farrugia, *WINGX, A Windows Program for Crystal Structure Analysis*, University of Glasgow, Glasgow, UK, 1988.
- (a) C. Lee, W. Yang and R. G. Parr, *Phys. Rev. B*, 1998, **37**, 785; (b) A. D. Becke, *J. Chem. Phys.*, 1993, **98**, 5648.
- M. J. Frisch, G. W. Trucks, H. B. Schlegel, G. E. Scuseria, M. A. Robb, J. R. Cheeseman, G. Scalmani, V. Barone, B. Mennucci, G. A. Petersson, H. Nakatsuji, M. Caricato, X. Li, H. P. Hratchian, A. F. Izmaylov, J. Bloino, G. Zheng, J. L. Sonnenberg, M. Hada, M. Ehara, K. Toyota, R. Fukuda, J. Hasegawa, M. Ishida, T. Nakajima, Y. Honda, O. Kitao, H. Nakai, T. Vreven, J. A. Montgomery, Jr, J. E. Peralta, F. Ogliaro, M. Bearpark, J. J. Heyd, E. Brothers, K. N. Kudin, V. N. Staroverov, R. Kobayashi, J. Normand, K. Raghavachari, A. Rendell, J. C. Burant, S. S. Iyengar, J. Tomasi, M. Cossi, N. Rega, J. M. Millam, M. Klene, J. E. Knox, J. B. Cross, V. Bakken, C. Adamo, J. Jaramillo, R. Gomperts, R. E. Stratmann, O. Yazyev, A. J. Austin, R. Cammi, C. Pomelli, J. W. Ochterski, R. L. Martin, K. Morokuma, V. G. Zakrzewski, G. A. Voth, P. Salvador, J. J. Dannenberg, S. Dapprich, A. D. Daniels, O. Farkas, J. B. Foresman, J. V. Ortiz, J. Cioslowski and D. J. Fox, *Gaussian 09, Revision A.01*, Gaussian, Inc., Wallingford CT, 2009.
- (a) P. K. Lee, H. W. Liu, S. M. Yiu, M. W. Louie and K. K. W. Lo, *Dalton Trans.*, 2011, **40**, 2180; (b) G. G. Shan, H. B. Li, Z. C. Mu, D. X. Zhu, Z. M. Su and Y. Liao, *J. Organomet. Chem.*, 2012, **702**, 27.
- (a) N. Zhao, Y. H. Wu, H. M. Wen, X. Zhang and Z. N. Chen, *Organometallics*, 2009, **28**, 5603; (b) H. F. Chen, K. T. Wong, Y. H. Liu, Y. Wang, Y. M. Cheng, M. W. Chung, P. T. Chou and H. C. Su, *J. Mater. Chem.*, 2011, **21**, 768.
- (a) G. Volpi, C. Garino, L. Salassa, J. Fiedler, K. I. Hardcastle, R. Gobetto and C. Nervi, *Chem.–Eur. J.*, 2009, **15**, 6415; (b)

- S. Ladouceur, D. Fortin and E. Zysman-Colman, *Inorg. Chem.*, 2011, **50**, 11514.
- 23 (a) X. S. Zeng, M. Tavasli, I. F. Perepichka, A. S. Batsanov, M. R. Bryce, C. J. Chiang, C. Rothe and A. P. Monkman, *Chem.–Eur. J.*, 2008, **14**, 933; (b) Q. Zhao, S. J. Liu, M. Shi, C. M. Wang, M. X. Yu, L. Li, F. Y. Li, T. Yi and C. H. Huang, *Inorg. Chem.*, 2006, **45**, 6152.
- 24 (a) M. S. Lowry, W. R. Hudson, R. A. Pascal, Jr and S. Bernhard, *J. Am. Chem. Soc.*, 2004, **126**, 14129; (b) L. He, L. Duan, J. Qiao, R. J. Wang, P. Wei, L. D. Wang and Y. Qiu, *Adv. Funct. Mater.*, 2008, **18**, 2123.
- 25 (a) J. Li, P. I. Djurovich, B. D. Alleyne, M. Yousufuddin, N. N. Ho, J. C. Thomas, J. C. Peters, R. Bau and M. E. Thompson, *Inorg. Chem.*, 2005, **44**, 1713; (b) Q. Zhao, F. Y. Li, S. J. Liu, M. X. Yu, Z. Q. Liu, T. Yi and C. H. Huang, *Inorg. Chem.*, 2008, **47**, 9526; (c) C. H. Yang, J. Beltran, V. Lemaire, J. Cornil, D. Hartmann, W. Sarfert, R. Fröhlich, C. Bizzarri and L. De Cola, *Inorg. Chem.*, 2010, **49**, 9891.
- 26 (a) B. Chen, Y. H. Li, W. Yang, W. Luo and H. B. Wu, *Org. Electron.*, 2011, **12**, 766; (b) H. C. Su, F. C. Fang, T. Y. Hwu, H. H. Hsieh, H. F. Chen, G. H. Lee, S. M. Peng, K. T. Wong and C. C. Wu, *Adv. Funct. Mater.*, 2007, **17**, 1019.
- 27 (a) G. Kalyuzhny, M. Buda, J. McNeill, P. Barbara and A. J. Bard, *J. Am. Chem. Soc.*, 2003, **125**, 6272; (b) J. D. Slinker, J. S. Kim, S. Flores-Torres, J. H. Delcamp, H. D. Abruña, R. H. Friend and G. G. Malliaras, *J. Mater. Chem.*, 2007, **7**, 76.
- 28 (a) K. Chen, C. H. Yang, Y. Chi, C. S. Liu, C. H. Chang, C. C. Chen, C. C. Wu, M. W. Chung, Y. M. Cheng, G. H. Lee and P. T. Chou, *Chem.–Eur. J.*, 2010, **16**, 4315; (b) M. Abrahamsson, M. J. Lundqvist, H. Wolpher, O. Johansson, L. Eriksson, J. Bergquist, T. Rasmussen, H. C. Becker, L. Hammarström, P. O. Norrby, B. Åkermark and P. Persson, *Inorg. Chem.*, 2008, **47**, 3540.
- 29 H. J. Bolink, L. Cappelli, S. Cheylan, E. Coronado, R. D. Costa, N. Lardiés, M. K. Nazeeruddin and E. Ortí, *J. Mater. Chem.*, 2007, **17**, 5032.
- 30 (a) T. Tsukuda, M. Kawase, A. Dairiki, K. Matsumoto and T. Tsubomura, *Chem. Commun.*, 2010, **46**, 1905; (b) N. D. Ngugen, G. Q. Zhang, J. W. Lu, A. E. Sherman and C. L. Frase, *J. Mater. Chem.*, 2011, **21**, 8409; (c) H. Y. Li, X. Q. Zhang, Z. G. Chi, B. J. Xu, W. Zhou, S. W. Liu, Y. Zhang and J. R. Xu, *Org. Lett.*, 2011, **13**, 556; (d) J. Ni, X. Zhang, Y. H. Wu, L. Y. Zhang and Z. N. Chen, *Chem.–Eur. J.*, 2011, **17**, 1171.
- 31 (a) H. Bi, D. Chen, D. Li, Y. Yuan, D. Xia, Z. Zhang, H. Zhang and Y. Wang, *Chem. Commun.*, 2011, **47**, 4135; (b) X. Q. Zhang, Z. G. Chi, H. Y. Li, B. J. Xu, X. F. Li, W. Zhou, S. W. Liu, Y. Zhang and J. R. Xu, *Chem.–Asian J.*, 2011, **6**, 808; (c) Y. Sagara, T. Mutai, I. Yoshikawa and K. Araki, *J. Am. Chem. Soc.*, 2007, **129**, 1520.